

# Lawrence Berkeley National Laboratory

## Lawrence Berkeley National Laboratory

### **Title**

REGROWTH BEHAVIOR OF THREE DIFFERENT DAMAGE STRUCTURES IN P+ IMPLANTED AND SUBSEQUENTLY LASER ANNEALED Si

### **Permalink**

<https://escholarship.org/uc/item/7s51s936>

### **Author**

Sadana, D.K.

### **Publication Date**

1979-10-01



# Lawrence Berkeley Laboratory

UNIVERSITY OF CALIFORNIA

## Materials & Molecular Research Division

To be published in the Proceedings of the Electrochemical Society, Inc.,  
Los Angeles, CA, October 14-19, 1979

REGROWTH BEHAVIOR OF THREE DIFFERENT DAMAGE STRUCTURES IN  
 $P^+$  IMPLANTED AND SUBSEQUENTLY LASER ANNEALED Si

D. K. Sadana, M. C. Wilson, G. R. Booker, and J. Washburn

October 1979

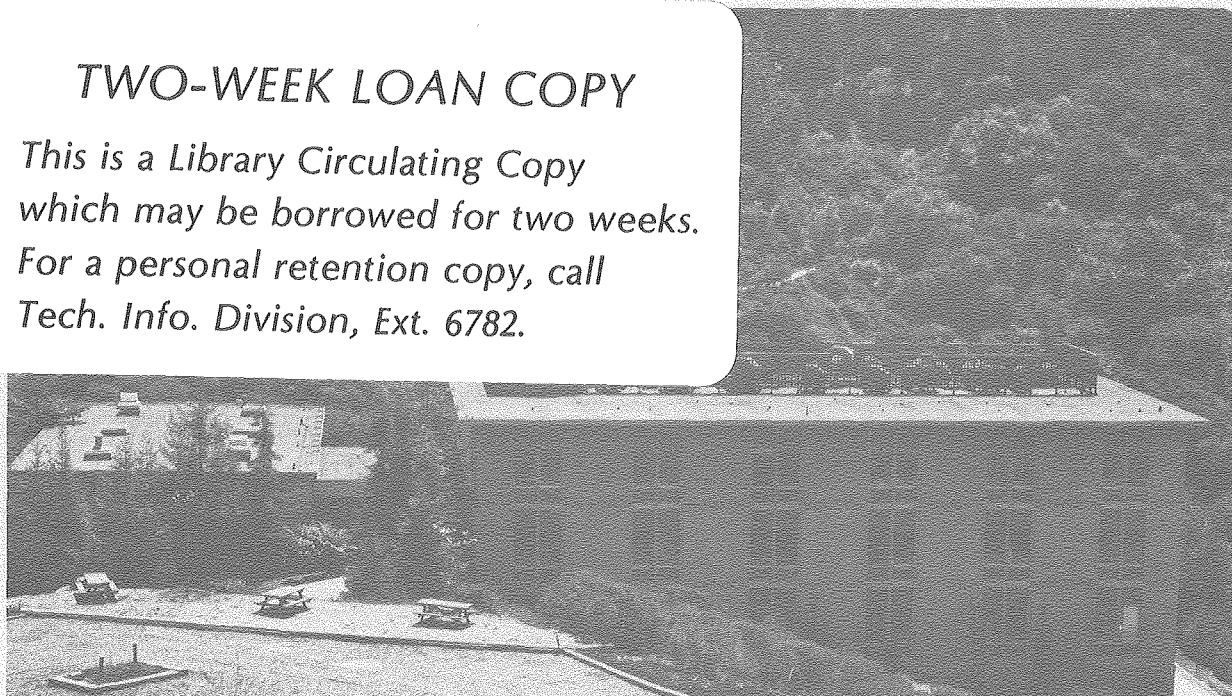
RECEIVED  
LAWRENCE  
BERKELEY LABORATORY

DEC 18 1979

LIBRARY AND  
DOCUMENTS SECTION

### TWO-WEEK LOAN COPY

*This is a Library Circulating Copy  
which may be borrowed for two weeks.  
For a personal retention copy, call  
Tech. Info. Division, Ext. 6782.*



*LBL-10008 c.2*

## DISCLAIMER

This document was prepared as an account of work sponsored by the United States Government. While this document is believed to contain correct information, neither the United States Government nor any agency thereof, nor the Regents of the University of California, nor any of their employees, makes any warranty, express or implied, or assumes any legal responsibility for the accuracy, completeness, or usefulness of any information, apparatus, product, or process disclosed, or represents that its use would not infringe privately owned rights. Reference herein to any specific commercial product, process, or service by its trade name, trademark, manufacturer, or otherwise, does not necessarily constitute or imply its endorsement, recommendation, or favoring by the United States Government or any agency thereof, or the Regents of the University of California. The views and opinions of authors expressed herein do not necessarily state or reflect those of the United States Government or any agency thereof or the Regents of the University of California.

REGROWTH BEHAVIOR OF THREE DIFFERENT DAMAGE STRUCTURES  
IN P<sup>+</sup> IMPLANTED AND SUBSEQUENTLY LASER ANNEALED Si

D. K. Sadana,\* M. C. Wilson,<sup>†</sup> G. R. Booker,<sup>†</sup>  
and J. Washburn\*

\*Lawrence Berkeley Laboratory  
University of California  
Berkeley, California 94720

<sup>†</sup>Department of Metallurgy  
University of Oxford  
Oxford OX1 3PH, England

ABSTRACT

The aim of the work was to study the regrowth behavior of three different damage structures, namely, a buried amorphous layer, a continuous amorphous layer extending from the surface of the specimen and <sup>a</sup>buried layer of clusters in P<sup>+</sup> implanted (111) Si. These structures were obtained by implanting P<sup>+</sup> at 120 KeV to doses of  $5 \times 10^{14}$ ,  $10^{15}$  and  $5 \times 10^{15}/\text{cm}^2$  at implantation temperatures RT, 150° and 350°C respectively. A Q-switched ruby laser with a wavelength of 0.695 nm and at an energy either  $0.7\text{J}/\text{cm}^2$  or  $1.5\text{J}/\text{cm}^2$  was used for laser annealing. TEM was used to examine the damage in a 90° 'cross-sectional' view. At  $0.7\text{J}/\text{cm}^2$ , two-thirds of the continuous amorphous layer regrew to give a polycrystalline layer. The buried amorphous layer regrew leaving dislocation loops and clusters and the buried layer of clusters remained unaffected. However, at  $1.5\text{J}/\text{cm}^2$ , dislocations and stacking faults extended from the surface for all the structures and were in direct contact with the deeper lying damage containing clusters. The density of dislocations, stacking faults and

deeper lying clusters progressively increased with the dose of the implanted phosphorus.

## INTRODUCTION

The potential applications of high energy pulsed laser beams for the regrowth of damage layers in ion implanted semiconductors has drawn world-wide interest because of the simplicity of the process. By suitable choice of laser parameters, such as the energy, pulse length, etc, epitaxial regrowth of the damage layers resulting from implantation can, in principle, be carried out either in the solid phase or molten phase (1-3). However, the mechanism of regrowth is not yet fully understood. The present study is therefore aimed at studying the regrowth behavior of three different types of damage structures in P<sup>+</sup> implanted Si resulting from pulsed laser annealing at different energies. For all the work described here, TEM was used to examine the damage structures in 90° 'cross-sectional' and 'plan' views before and after the laser annealing. A mechanism for the regrowth has been suggested based on the observations made here.

## EXPERIMENTAL

a. Implantation. P-type 17 ohm-cm (111) Si wafers of 5 cm diameter were implanted in a non-channelling direction with 120 KeV P<sup>+</sup> ions using doses of either  $5 \times 10^{14}$ ,  $10^{15}$  or  $5 \times 10^{15}/\text{cm}^2$ . The implantation energy of 120 KeV corresponded to an LSS projected range of 1510

$\pm 690 \text{ \AA}$ . The implantation time in all instances was 10 minutes. The implantation temperatures in the three cases were RT,  $150^\circ$ , and  $350^\circ\text{C}$ . The increases above RT in the latter two cases being due to ion beam heating.

b. Laser. A Q-switched ruby laser operating at a wavelength of  $0.695 \text{ nm}$  was used. The multiple beam output was passed through a diffusing screen coupled to a light guide in order to achieve a flat and uniform intensity distribution (4). The laser energies of  $0.7\text{J}/\text{cm}^2$  and  $1.5\text{J}/\text{cm}^2$  were used for each specimen. The pulse length for all the specimens was  $\sim 30 \text{ n sec}$ .

c. TEM. For TEM studies,  $90^\circ$  'cross-section' and 'plan' view specimens were prepared. The 'cross-section' specimens were obtained by cleaving the slices and then mechanically polishing followed by low energy ion-beam thinning as described previously (5). The micrographs from these specimens correspond to the  $(\bar{1}\bar{1}0)$  plane perpendicular to the original  $(111)$  specimen surface plane. All of the TEM examinations described here were performed using bright-field strong-beam diffraction contrast conditions. Transmission electron diffraction (TED) patterns were also obtained to aid in the identification of the damage, using either the standard selected area method or microdiffraction techniques.

## RESULTS

a. Buried Amorphous Layer. For the specimen implanted to a dose of  $5 \times 10^{14}/\text{cm}^2$ , the TEM 'cross-section' micrograph showed a  $\sim 1150 \text{ \AA}$  wide buried amorphous layer 'A' located at a mean depth of  $\sim 850 \text{ \AA}$  from the surface (Fig. 1a). The region between the surface and the top edge of damage layer 'A' had sparsely distributed clusters.

After the specimen had been laser annealed at  $0.7 \text{ J}/\text{cm}^2$ , the region between the surface and  $\sim 1600 \text{ \AA}$  depth, marked as 'B' in Fig. 1b, consisted of dislocation loops (mean diameter  $\sim 100 \text{ \AA}$ ) and clusters. The density of dislocation loops obtained from 'plan' view micrograph (not included in the text) was  $\sim 6 \times 10^{10}/\text{cm}^2$ . The regrown region 'B' was followed by a second damage layer 'C'  $\sim 250 \text{ \AA}$  wide, consisting of dense fine structure and was located at a depth immediately below the bottom edge of layer 'A' in the as implanted specimen (Fig. 1b).

After the specimen had been laser annealed at  $1.5 \text{ J}/\text{cm}^2$ , the first damage layer 'B' in the previous specimen was no longer present. The previous second layer 'C' was much less in evidence and consisted mainly of small damage clusters in the layer 'D' (Fig. 1c). Occasionally, single dislocations extending from the surface to the clusters layer were observed.

b. Continuous Amorphous Layer. For the wafers implanted to a dose of  $10^{15}/\text{cm}^2$ , the TEM 'cross-section' micrographs showed a continuous amorphous layer 'E' extending from the surface to a depth of  $\sim 1800 \text{ \AA}$ . At the lower edge of this layer there was a narrow irregular

zone  $\sim 250 \text{ \AA}$  wide corresponding to heavily damaged but not amorphous material (the narrow dark layer in Fig. 2a).

After the specimen had been annealed at  $0.7 \text{ J/cm}^2$ , a first damage layer 'F' comprising polycrystalline material with mean grain size  $\sim 1000 \text{ \AA}$  extended from the specimen surface to a depth of  $1500 \text{ \AA}$  (Fig. 2b). A second damage layer 'G' consisting of dense fine structure and  $\sim 500 \text{ \AA}$  wide occurred and was in direct contact with the first damage layer (6).

After the specimen had been laser annealed at  $1.5 \text{ J/cm}^2$ , a first damage layer 'H' comprising single crystal material containing mainly stacking faults but also dislocations extended from the surface to a depth of  $\sim 1800 \text{ \AA}$  (Fig. 2c). The stacking faults density (from 'plan' view micrographs) at the surface was  $\sim 10^9/\text{cm}^2$ . A second damage layer 'I' consisting of dense fine structure and  $\sim 200 \text{ \AA}$  wide occurred and was in direct contact with the first damage layer.

c. Buried Clusters Layer. For the specimens implanted to a dose of  $5 \times 10^{15}/\text{cm}^2$ , the TEM 'cross-section' micrographs showed a buried layer of clusters 'J',  $\sim 1200 \text{ \AA}$  wide, in single crystal material that was located at a mean depth of  $\sim 2000 \text{ \AA}$  (Fig. 3a). There were 'visible damage' free regions on either side of layer 'J' (the term 'visible damage' refers to the damage visible by TEM). After the specimen had been laser annealed at  $0.7 \text{ J/cm}^2$ , no noticeable change in the damage structure or distribution occurred (Fig. 3b).



However, for the specimen laser annealed at  $1.5\text{J}/\text{cm}^2$ , the results were similar to that of  $10^{15}/\text{cm}^2$  except that the densities of dislocations and stacking faults (from 'plan' view micrographs) were now  $\sim 10^{10}/\text{cm}^2$  and  $\sim 7 \times 10^{11}/\text{cm}^2$ , respectively. The first damage layer containing stacking faults and dislocations is marked as 'L' and the second damage layer containing small clusters is marked as 'M' in Fig. 3c.

#### DISCUSSION

A striking feature of the laser annealing is that two distinctly different annealing zones are sometimes present within individual specimens (Figs. 2b, 2c and 3c). We suggest the following mechanism for the formation of the observed regrown structures.

For the as implanted specimens with buried damage layers (Fig. 1a and Fig. 3a), the near-surface region although damaged, is still single crystal as shown by TEDs (not included in the text). However, for the  $10^{15} \text{P}^+/\text{cm}^2$  specimen, the near-surface region is amorphous. As a result, the energy absorption in the 'buried layer' specimens occurred over a larger volume as compared to the 'continuous amorphous layer' specimen. This is because of different absorption coefficients for amorphous and single crystal Si. Therefore, at lower energies, i.e.,  $0.7\text{J}/\text{cm}^2$  the 'buried damage layers' either partially recover in solid phase (Fig. 1b) or remain unaffected (Fig. 3b) depending on the thickness and the extent of damage in the near-surface region. However, for 'continuous amorphous layers' strong absorption of energy nearer to the surface causes melting of the surface layer, but the deeper lying damage still anneals in the solid phase. The

molten upper layer in this case regrows on a heavily damaged or amorphous substrate forming the polycrystalline layer.

At  $1.5\text{J}/\text{cm}^2$ , the laser energy absorption is high enough to melt the main damage layer in all three specimens but the solidification of the molten material on deeper lying clusters still gives rise to the formation of the dislocations and stacking faults. The density of these clusters increases progressively with the dose of the implanted  $\text{P}^+$  ions. Consequently, the density of dislocations and stacking faults in the regrown layer also increases.

#### CONCLUSIONS

1. The regrowth structures from damaged layers in  $\text{P}^+$  implanted Si resulting from laser annealing at  $0.7\text{J}/\text{cm}^2$  critically depend on the crystallinity of the specimen in the near-surface region.
2. At a laser energy of  $1.5\text{J}/\text{cm}^2$ , the regrowth of the damage layer occurs via melting for all cases. The perfection of the regrown material then depends on the depth of melting relative to the depth of the original implantation damage.

## ACKNOWLEDGEMENTS

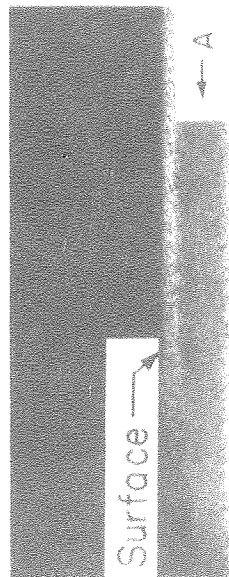
The authors would like to thank Dr. A. Cullis of RSRE Malvern (England) for laser annealing the Si specimens. The authors would like to acknowledge the financial support of the Department of Energy (USA) through Materials and Molecular Research Division of Lawrence Berkeley Laboratory, Berkeley, California and Science Research Council (UK) through Department of Metallurgy, Oxford.

## REFERENCES

1. G. K. Celler, J. M. Poate and L. C. Kimerling, *App. Phys. Lett.* 32, 464 (1978).
2. R. T. Young, C. W. White, G. J. Clark, J. Narayan, W. H. Christie, M. Murakami, P. W. King, and S. D. Kramer, *App. Phys. Lett.* 32, 139 (1978).
3. J. S. Williams, this proceeding.
4. A. G. Cullis, H. C. Webber and P. Bailey, *J. Phys. E.: Sci. Instrum.* 12, 688 (1979).
5. H. R. Pettit and G. R. Booker, *Proc. 25th Anniv. Meet., EMAG (IOP), London (1971)*.
6. D. K. Sadana, M. C. Wilson and G. R. Booker, *J. Microscopy*, 118 (1980).

## FIGURE CAPTIONS

- Fig. 1. TEM 'cross-section' micrographs showing the laser annealing sequence for P<sup>+</sup> implanted (111) Si. (Ti = RT, N<sub>P<sup>+</sup></sub> = 5X10<sup>14</sup>/cm<sup>2</sup>, E<sub>i</sub> = 120 KeV)
- Fig. 2. TEM 'cross-section' micrographs showing the laser annealing sequence for P<sup>+</sup> implanted (111) Si. Ti = 150°C, N<sub>P<sup>+</sup></sub> = 10<sup>15</sup>/cm<sup>2</sup>, E<sub>i</sub> = 120 KeV)
- Fig. 3. TEM 'cross-section' micrographs showing the laser annealing sequence for P<sup>+</sup> implanted (111) Si. (Ti = 350°C, N<sub>P<sup>+</sup></sub> = 5X10<sup>15</sup>/cm<sup>2</sup>, E<sub>i</sub> = 120 KeV)



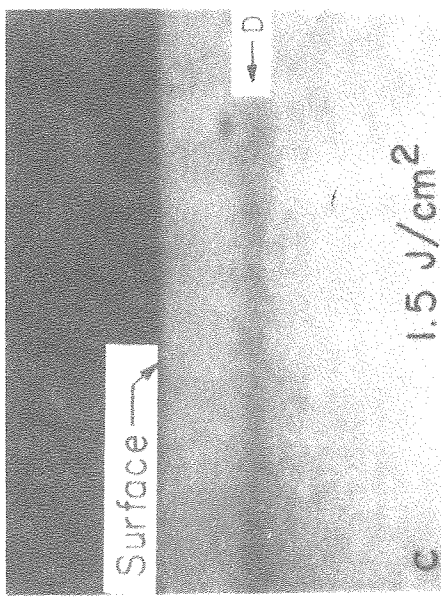
Ti = RT

a



0.7 J/cm<sup>2</sup>

b

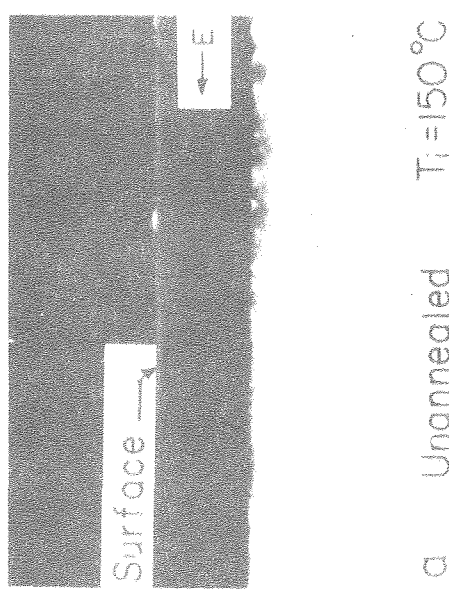
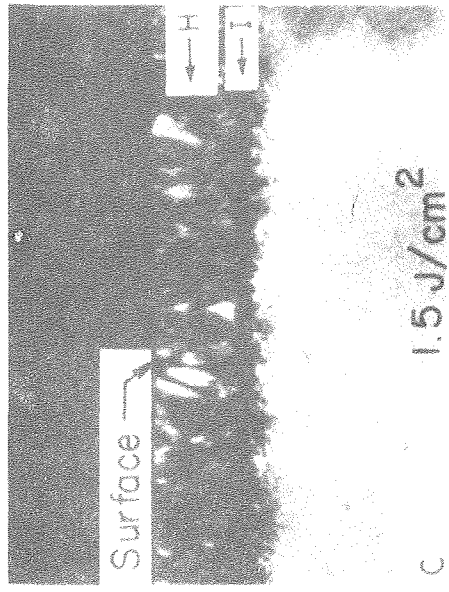


1.5 J/cm<sup>2</sup>

c

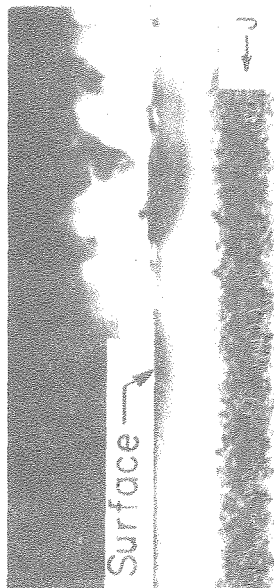
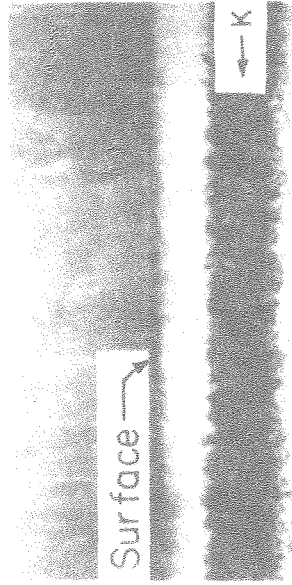
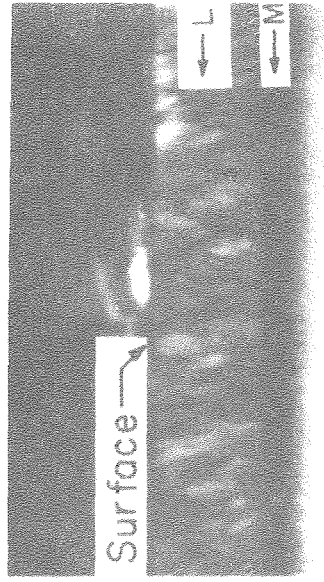
0.4 μm

XBB790-14333



0.4 μm

XBB790-14332



1.5 J/cm<sup>2</sup>

0.7 J/cm<sup>2</sup>

T<sub>j</sub> = 350°C

c

b

a

0.4 μm

XBB790-14331